Received: 9 August 2022 | Accepted: 8 January 2023

DOI: 10.1111/aos.15637

Acta Ophthalmologica

ORIGINAL ARTICLE

Imaging biomarkers of leukaemic choroidopathy

Matteo Menean[1,2] | **Aurelio Apuzzo**[1,2] | **Sara Mastaglio**[3] | **Massimo Bernardi**[3] | **Fabio Ciceri**[1,3] | **Giulio Modorati**[2] | **Elisabetta Miserocchi**[1,2] | **Francesco Bandello**[1,2] | **Maria Vittoria Cicinelli**[1,2]

[1]School of Medicine, Vita-Salute San Raffaele University, Milan, Italy

[2]Department of Ophthalmology, IRCCS San Raffaele Scientific Institute, Milan, Italy

[3]Hematology and Bone Marrow Transplant Unit, IRCCS San Raffaele Scientific Institute, Milan, Italy

Correspondence
Maria Vittoria Cicinelli, Department of Ophthalmology, IRCCS San Raffaele Scientific Institute, Via Olgettina 60, Milan 20132, Italy.
Email: cicinelli.mariavittoria@hsr.it

Abstract

Purpose: To longitudinally investigate choroidal and choriocapillaris perfusion metrics and the number of choroidal hyperreflective foci (HRF) in patients with acute leukaemia (AL) before and after disease remission and to correlate these metrics with systemic parameters during active disease.

Methods: Prospective, longitudinal study of 26 eyes of 14 AL patients. All patients underwent optical coherence tomography (OCT) and OCT-angiography (OCTA) in the acute phase. Subfoveal choroidal thickness (CT), total, luminal and stromal choroidal area (TCA, LCA, SCA), choroidal vascularity index (CVI), choriocapillaris flow deficits (cFD) density, and choroidal HRF number were computed. In a subset, the measurements were repeated after AL remission. Age- and gender-matched 26 healthy controls were recruited for cross-sectional comparisons.

Results: Patient's mean age was 59 ± 12 years. The TCA, LCA, SCA and choroidal HRF number were significantly higher in patients than controls ($p = 0.028$, $p = 0.044$, $p = 0.024$ and $p = 0.001$, respectively). Lower haemoglobin levels were associated with lower CT ($r = 0.58$, $p = 0.008$). Higher D-dimer values were associated with lower TCA ($r = -0.52$, $p = 0.008$), lower LCA ($r = -0.50$, $p = 0.006$), higher cFD density ($r = 0.41$, $p = 0.044$) and higher choroidal HRF number ($r = 0.47$, $p = 0.008$). The CT, TCA, SCA and choroidal HRF number significantly reduced after AL remission ($p = 0.001$, $p = 0.047$, $p = 0.007$ and $p = 0.002$ respectively). The CVI increased significantly compared to the active phase ($p = 0.013$).

Conclusion: The study demonstrates a subclinical choroidal involvement in patients with AL, with relative stromal thickening in the acute phase, and normalization after disease remission. Choroidal HRF were identified as a biomarker of leukaemic choroidopathy. Choriocapillaris and choroidal vascularity were inversely correlated with a systemic pro-coagulant state.

KEYWORDS

acute leukaemia, choriocapillaris, choroidal hyperreflective foci, choroidal vascularity index, flow deficits, leukaemic choroidopathy

1 | INTRODUCTION

Acute leukaemia (AL) is an early blood-forming cell cancer with intravascular and medullary involvement, rarely localizing in solid organs (González-Herrero et al., 2018). Leukaemic cells can be delivered to every organ through systemic circulation, including the eye (Bakst et al., 2020; Devine & Larson, 1994). Among the ocular structures, the choroid is one of the preferential sites for AL cells homing (Davis, 2013), with virtually all cases presenting with choroidal infiltration in postmortem studies (Leonardy et al., 1990).

Noninvasive imaging has allowed objective evaluation of the choroid in healthy and diseased eyes. Choroidal luminal and stromal components have been measured on optical coherence tomography (OCT), and their ratio, expressed as choroidal vascularity index (CVI), has been deployed in ocular and systemic conditions (Byon et al., 2020; Iovino et al., 2020; Nicolini et al., 2022). Choriocapillaris flow deficits (FD) have been quantified with OCT angiography (OCTA) (Zhang et al., 2018). Qualitative features have also been described; choroidal hyperreflective foci (HRF) have been interpreted as intrachoroidal leukocytes (Kim & Oh, 2022; Romano et al., 2020).

An in vivo characterization of choroidal changes in AL is currently lacking. This study aimed to fill this knowledge gap. Firstly, we compared the choroidal perfusion metrics between AL patients and healthy controls and explored their correlations with systemic haematological parameters. Then, we investigated the choroidal changes before and after disease remission. With the hypothesis that HRF may represent an indirect sign of leukaemic choroidopathy, we also included the assessment of HRF in our analyses.

2 | METHODS

This was a prospective, longitudinal study on AL patients treated at the Haematology and Bone Marrow Transplant Unit of San Raffaele Scientific Institute, Milano (Italy) from March 2021 to December 2021. We conducted the study under the tenets of the Declaration of Helsinki, and we obtained written informed consent from each patient. We included patients affected by myeloid or lymphoblastic AL, diagnosed based on morphological, cytogenetical, immune-phenotypical and molecular studies on the bone marrow aspirate. We excluded eyes with optic media opacities, retinal or optic disc tumour infiltration, or other concurrent ocular diseases.

We performed a complete ophthalmic examination, including visual acuity (VA) measurement and multimodal imaging, during the active phase of AL before systemic chemotherapy was started or within the first days of induction therapy. We collected age, gender, medical and ocular history, and systemic laboratory parameters, namely white blood cells (WBC) [$*10^9$/L], circulating blasts [%], haemoglobin [g/dl], haematocrit [%], platelets [$*10^9$/L], fibrinogen [mg/dl], cross-linked fibrin degradation products (D-dimer) [μg/ml], international normalized ratio (INR) and activated partial thromboplastin time (APTT) ratio.

All patients underwent systemic chemotherapy at the Haematology and Bone Marrow Transplant Unit. Patients underwent bone marrow biopsy 1 month after consolidation therapy to confirm AL remission, defined by a total or partial reduction in the bone marrow blasts' count below the threshold of 5%. Patients with AL remission were re-examined the same days they were hospitalized for bone marrow biopsy.

We recruited an age- and gender-matched healthy subject as a control for each included eye.

2.1 | Imaging protocol

We performed a single-line horizontal spectral-domain OCT (SD-OCT) with enhanced-depth imaging modality (Spectralis HRA+OCT, Heidelberg Engineering, Germany), ultra-widefield pseudocolor fundus photography (Optos Silverstone PLC; Dunfermline, UK), and a $3\times3\,mm^2$ OCTA (RTVue-XR Avanti system, Optovue Inc., Fremont, CA, USA) centred on the fovea. Structural SD-OCT scans were acquired after averaging 25 SD-OCT B-scans.

We exported the structural SD-OCT scans and the OCTA slabs as JPEGs. We analysed all the images with the free software ImageJ (National Institutes of Health, Bethesda, MD, USA).

2.2 | Choroidal measurements

On SD-OCT scans, we manually measured the subfoveal choroidal thickness (CT) as the distance between Bruch's membrane and the sclero-choroidal junction under the foveal depression. We measured the total (TCA), the luminal (LCA) and the stromal choroidal area (SCA) in a 1500-μm wide region centred on the fovea. We selected the TCA as a 1500-μm polygon having Bruch's membrane as the superior boundary and the sclero-choroidal junction as the inferior boundary. We selected the LCA using the colour threshold tool (hue and saturation bars set on 0–255, brightness bars set on 0 and 254) after binarizing each SD-OCT scan with the *Niblack* autolocal threshold. We calculated the CVI as the ratio between the LCA and the TCA. We derived the SCA as the difference between the TCA and the LCA (Betzler et al., 2022).

We identified HRF as round or diamond-shaped dots with hyperreflective signal on B-scan SD-OCT scans. To ensure a standardized and reproducible method for HRF count, we set a reflectivity threshold, selecting those pixels with a signal brightness of at least 2 standard deviations (SD) above the mean choroidal brightness (Corradetti et al., 2019; Kim & Oh, 2022; Nassisi et al., 2018). As a preliminary step, we corrected the choroidal signal intensity for any potential attenuation by optic media opacity normalizing all SD-OCT images according to vitreous and the retinal pigment epithelium (RPE) mean brightness (Figure 1a). This adjustment was fundamental to avoid hyper- or hyporeflectivity due to shadowing artefacts. All images were normalized, assuming the vitreous and RPE brightness to be 0 (black) and 255 (white) respectively. We measured the mean vitreous brightness in a 1500×1500-μm square area upon the fovea through the imageJ histogram tool. We subtracted the obtained value from the whole image intensity using the subtract tool (Process → Math → Subtract). Then, we divided each pixel's brightness by the mean RPE brightness, measured in a 1500-μm wide region under the fovea, according to the following formula: RPE mean brightness/white (255) (Borrelli et al., 2017). After normalization of the OCT scan brightness (Figure 1b), we manually segmented the choroidal area with the polygon selection tool, using the RPE as the superior, the sclero-choroidal junction as the inferior, and the scan margins as lateral boundaries (Figure 1c). Then, we cleared the image outside the selected region of interest.

To highlight HRF, we computed the mean choroidal brightness using the histogram tool and subtracted the mean brightness +2 SD (Figure 1d) (Corradetti et al., 2019; Kim & Oh, 2022; Nassisi et al., 2018). We increased the image contrast with the enhance contrast tool (0.3% of saturated pixels) (Figure 1e), and we binarized the resulting image using the *Phalsankar*

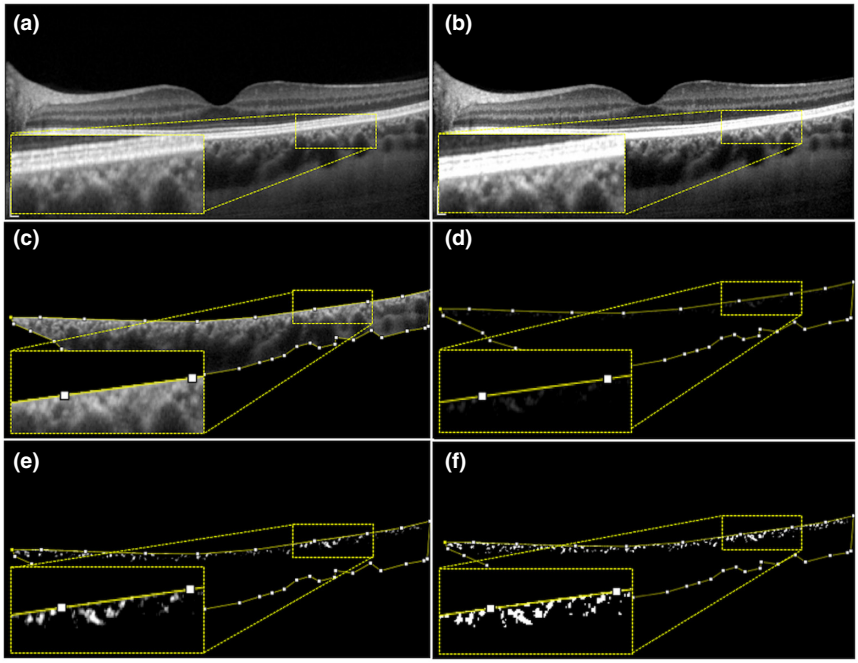

FIGURE 1 Normalization of spectral domain optical coherence tomography (SD-OCT) image and choroidal HRF count. (a) 8-bit SD-OCT image. (b) 8-bit SD-OCT image normalized according to vitreous and retinal pigmented epithelium (RPE) mean brightness. (c) Manually segmented choroidal area. (d) Manually segmented choroidal area. Each pixel has 2 standard deviations (SD) subtracted brightness compared to the previous image (c). (e) Manually segmented choroidal area. Increase contrast tool (0.3% of saturated pixels) has been applied. (f) Binarization of the previous image (e) through *Phalsankar* autolocal threshold, with a preset radius of 4 pixels.

autolocal threshold with a preset radius of 4 pixels (Figure 1f). We automatically counted the number of choroidal HRF with the Analyse particles function (Corradetti et al., 2019, Kim & Oh, 2022, Nassisi et al., 2018).

We tested the consistency of our HRF counting method by computing the inter-rater agreement between two independent raters (MM and AA). We used with intraclass correlation coefficient (ICC) with a two-way random-effects model (Koo & Li, 2016). The ICC was moderate (ICC = 0.72, 95% CI 0.56 to 0.83), and we used the averaged HRF counts between the two readers for subsequent analyses.

2.3 | Choriocapillaris measurements

We measured the FD density in a 20-μm-thick choriocapillaris slab, automatically generated by the OCTA software (TVue XR AngioVue Optical Coherence Tomography Angiography Software) (Nesper et al., 2021) to be consistent with the previous literature using the same device. To reduce the shadow effect from the overlying large intraretinal vessels, we generated a mask from the superficial retinal capillary plexus through *max entropy* thresholding (Figure S1a, b), and we subtracted the mask from the choriocapillaris slab (Figure S1c). We binarized the obtained image with the *Phalsankar* autolocal threshold with a preset 4-pixel radius (Figure S1d), and we automatically counted the area with no flow signal with the analyse particle tool. We corrected the FD density (cFD density) by subtracting the applied mask from the entire slab area, according to the formula:

$$\left(\frac{\text{Flow Deficit Area}}{3000\times 3000-\text{Mask Area}}\right)*100\,[\%].$$

2.4 | Statistical analysis

We performed all statistical analyses by setting a threshold for statistical significance at $p<0.05$. We summarized continuous variables as their mean ± SD if normally distributed or as their median and interquartile range (IQR) otherwise. We summarized categorical variables as their absolute and relative prevalence.

As per the primary aim, we investigated differences in CT, TCA, LCA, SCA, CVI, cFD density and choroidal HRF number between AL and control eyes using linear mixed models where each quantitative metric was the dependent variable, the group (AL vs. control) was the fixed effect. The patients' identification number was the random effect to account for intrasubject correlations for both eyes' inclusion. We reported regression estimates and their 95% confidence intervals (CI).

As per the secondary aim, we explored correlations between the choroidal metrics, namely CT, TCA, LCA, SCA, CVI, cFD density and choroidal HRF, and laboratory findings (WBC, circulating blasts, haemoglobin, haematocrit, platelets, fibrinogen, D-dimer, INR, and APTT ratio) in AL patients using Pearson's correlations, and we reported correlation coefficients (r) and their 95% CI.

Finally, we investigated the longitudinal changes in choroidal perfusion metrics and choroidal HRF number within patients who reached AL remission using linear mixed models, where both the eye' and the patients' identification numbers were the nested random effects to account for intraeye and intrasubject correlations.

3 | RESULTS

Twenty-six eyes of 14 AL patients (9 males, 64%; mean age 59 ± 12 years) and 26 control eyes of 26 from 13 healthy volunteers were included. Two eyes of two patients were excluded because of retinal co-morbidities. Namely, one eye was excluded due to branch retinal arterial occlusion and the other due to previous retinal detachment treated with trans pars plana vitrectomy. Eleven patients (79%) had a new diagnosis of AL, three patients (11%) were studied at the time of disease relapse. None of the 14 patients had ocular symptoms, and the VA was 20/20 in all eyes. The cohort overlaps with a previous paper from our group investigating retinal circulation in AL (Cicinelli et al., 2022).

Clinically visible leukaemic retinopathy was observed in seven eyes of five patients (27%). Specifically, cotton wool spots were found in six eyes, mid-peripheral blot haemorrhages in two eyes and peripapillary splinter haemorrhages in one. None of the 26 eyes had signs of leukaemic retinopathy within the macula, potentially influencing the quality of the images.

3.1 | Choroidal and choriocapillaris metrics between AL patients and healthy controls

The TCA (1.65 ± 0.43 mm^2 vs. 1.38 ± 0.41 mm^2, $p = 0.028$), the LCA (1.06 ± 0.27 mm^2 vs. 0.91 ± 0.26 mm^2, $p = 0.044$) and the SCA (0.59 ± 0.19 mm^2 vs. 0.48 ± 0.17 mm^2, $p = 0.024$) were significantly higher in AL eyes than controls. On the contrary, the subfoveal CT, the CVI and the cFD density did not significantly differ between the two groups (Table 1). No significant differences in the choroidal metrics were found between eyes with leukaemic retinopathy and those without retinopathy (all $p > 0.05$).

The choroidal HRF were more numerous in the patients' group (88 ± 24 vs. 67 ± 15, $p = 0.001$). Choroidal HRF were predominantly arranged superficially in the choroid, presumably in the Sattler's layer, and clustered in the stromal area around small vessels. They did not show a preferential disposition between the subfoveal and the extrafoveal area (Figure S2). In the AL group, there was an association between the number of choroidal HRF and the TCA (regression estimate = 24.9 for each TCA mm^2 increase, 95% CI 3.00 to 40.7, $p = 0.001$) and the SCA (regression estimate = 49.7 for each SCA mm^2 increase, 95% CI 10.9 to 91.4, $p = 0.01$), but not with the LCA (regression estimate = 23.7 for each LCA mm^2 increase, 95% CI −5.36 to 48.05, $p = 0.06$). No significant correlation was found in the control group.

3.2 | Correlation between choroidal metrics and haematological and biochemical parameters

The haemoglobin levels were positively associated with the CT ($r = 0.58$, 95% CI 0.18 to 0.81, $p = 0.008$). The D-dimer was inversely related to TCA ($r = -0.52$, 95% CI −0.77 to −0.15, $p = 0.008$) and LCA ($r = -0.50$, 95% CI −0.75 to −0.12, $p = 0.006$), and positively associated with cFD density ($r = 0.41$, 95% CI 0.02 to 0.70, $p = 0.044$) and choroidal HRF number ($r = 0.47$, 95% CI 0.06 to 0.72, $p = 0.008$).

A higher cFD density was associated with a higher WBC count ($r = 0.45$, 95% CI 0.04 to 0.67, $p = 0.036$). No other correlations were found among the remaining laboratory tests and choroidal metrics (Table S1).

3.3 | Longitudinal analysis after AL remission

Ten eyes of five patients reached AL remission and were re-imaged after a median of 4 months (IQR 2–6 months). The subfoveal CT (367 ± 88 μm vs. 303 ± 72 μm, $p = 0.001$), the TCA (1.86 ± 0.31 mm^2 vs. 1.65 ± 0.35 mm^2, $p = 0.047$), the SCA (0.70 ± 0.15 mm^2 vs. 0.58 ± 0.14 mm^2, $p = 0.007$) and the number of choroidal HRF (75 ± 23 vs. 47 ± 11, $p = 0.002$) significantly reduced after clinical AL remission (Table 2; Figure 2). The CVI increased significantly compared to the active phase (0.65 ± 0.01 vs. 0.63 ± 0.03, $p = 0.013$). The cFD density and the LCA did not change significantly on longitudinal exams.

Postremission subfoveal CT, TCA, LCA, SCA, cFD density and choroidal HRF count were similar to the control group values.

TABLE 1 Choroidal parameters in patients with acute leukaemia and controls.

	Acute leukaemia patients ($n = 26$ eyes)	Controls ($n = 26$ eyes)	p-value
Subfoveal CT (μm)	330 ± 82	275 ± 73	0.156
TCA (mm^2)	1.65 ± 0.43	1.38 ± 0.41	0.028*
LCA (mm^2)	1.06 ± 0.27	0.91 ± 0.26	0.044*
SCA (mm^2)	0.59 ± 0.19	0.48 ± 0.17	0.024*
CVI	0.64 ± 0.04	0.66 ± 0.04	0.228
cFD density (%)	27.87 ± 2.77	27.89 ± 3.05	0.976
Choroidal HRF (n)	88 ± 24	67 ± 15	0.001*

Abbreviations: cFD, corrected flow deficits; CT, choroidal thickness; CVI, choroidal vascular index; HRF, hyperreflective foci; LCA, luminal choroidal area; SCA, stromal choroidal area; TCA, total choroidal area.

*Statistically significant data ($p < 0.05$).

TABLE 2 Choroidal parameters in patients with active acute leukaemia and after clinical remission.

	Active leukaemia	Post leukaemia remission	p-value
Subfoveal CT (μm)	367 ± 88	303 ± 72	0.001*
TCA (mm^2)	1.86 ± 0.31	1.65 ± 0.35	0.047*
LCA (mm^2)	1.16 ± 0.18	1.08 ± 0.22	0.210
SCA (mm^2)	0.70 ± 0.15	0.58 ± 0.14	0.007*
CVI	0.63 ± 0.03	0.65 ± 0.01	0.013*
cFD density (%)	27.89 ± 3.0	28.68 ± 2.89	0.307
Choroidal HRF (n)	75 ± 23	47 ± 11	0.002*

Abbreviations: cFD, corrected flow deficit; CT, choroidal thickness; CVI, choroidal vascular index; HRF, hyperreflective foci; LCA, luminal choroidal area; SCA, stromal choroidal area; TCA, total choroidal area.

*Statistically significant data ($p < 0.05$).

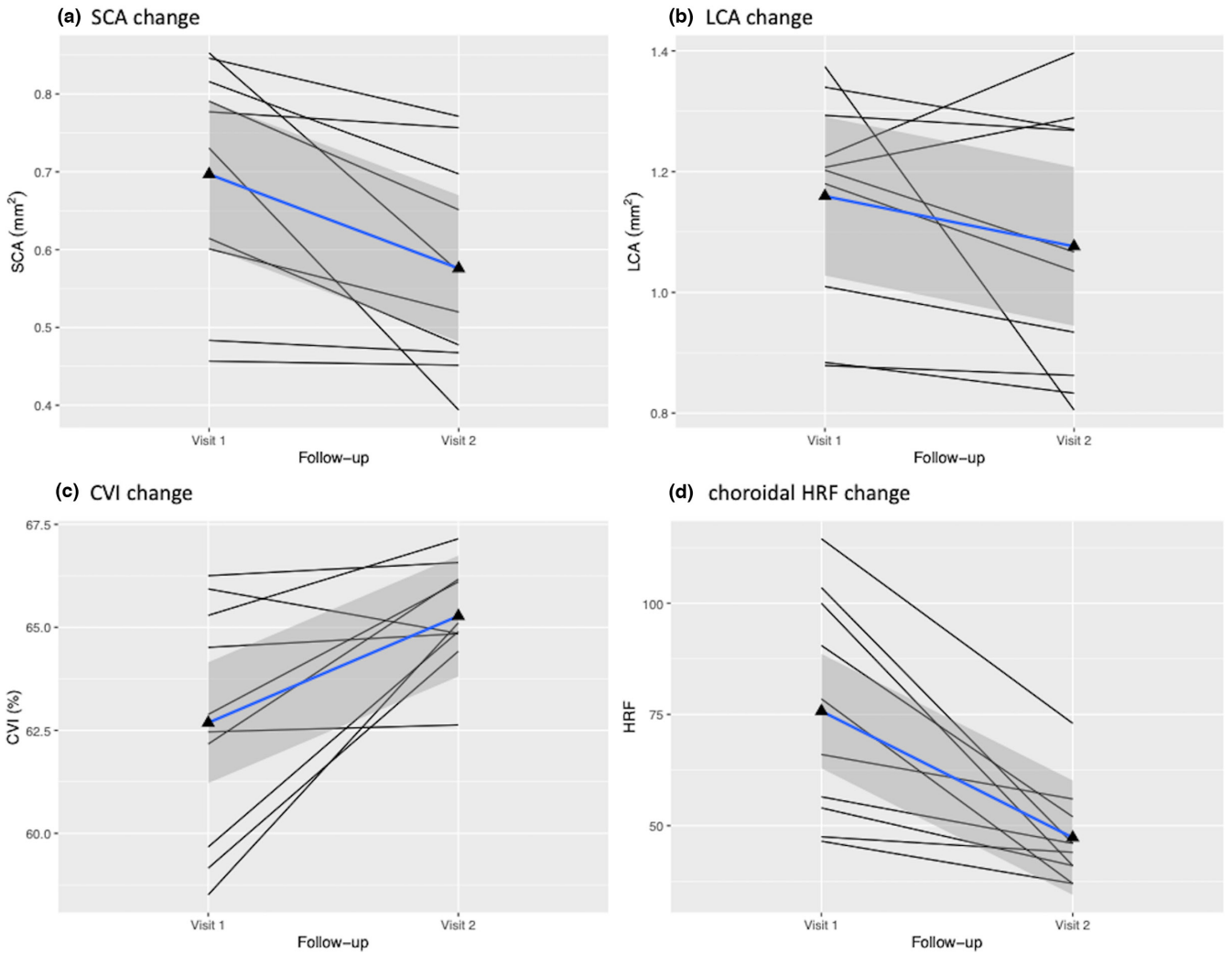

FIGURE 2 Comparison of choroidal vascular metrics and choroidal hyperreflective foci (HRF) in patients with AL during active phase of leukaemia (visit 1) and after AL clinical remission (visit 2). (a, b) The linear graphs show an overall decrease in stromal (SCA) and luminal (LCA) choroidal area. (c) The linear graph shows an overall increase in choroidal vascularity index (CVI). (d) The linear graph shows an overall decrease in choroidal HRF. Each solid black line indicates one eye. The blue line indicates the mean value. The grey-shadowed area shows the confidence interval of the mean value.

4 | DISCUSSION

This study longitudinally investigated the choroidal metrics in patients with AL by means of SD-OCT and OCTA and their correlations with systemic parameters. To date, it is the first in vivo deep characterization of choroidal involvement in patients with AL. We found patients with AL in their active phase had higher luminal and stromal choroidal areas than healthy subjects and more numerous choroidal HRF. The choriocapillaris was only marginally involved in the active disease, although our data suggest an inverse correlation between choriocapillaris perfusion, leukocytosis and procoagulant state.

The choroid is a privileged homing site of leukaemic cells (Dick & Lapidot, 2005). Leonardy et al. (1990) analysed postmortem eyes of patients with leukaemia and reported 93% of them had choroidal infiltration. Allen & Straatsma (1961) examined the eyes of 76 patients who died from leukaemia and reported an 89% rate of choroidal involvement. Although a diffuse choroidal thickening on SD-OCT has been described in patients with leukaemia (Bajenova et al., 2012; Choi, 2020; Coupland & Damato, 2008; Takita et al., 2018; Vieira et al., 2015), available imaging studies are mostly anecdotal. None included a quantitative analysis of the choroid and the choriocapillaris.

In our study, we separately investigated the different choroidal components, and we found patients with active AL had supranormal values of SCA, LCA and TCA. While the LCA remained unchanged, the SCA significantly reduced after disease remission, suggesting the largest changes in active AL occurred in the choroidal stroma. Postmortem studies of AL patients reported mottled thickening of the choroid and sheets of neoplastic cells in the innermost stromal interstices (Allen & Straatsma, 1961), more abundant at the posterior pole (Leonardy et al., 1990). In accordance with histopathology descriptions, we hypothesize that the reversible increase in the SCA values could be related to neoplastic infiltration. Other plausible alternatives, however, include an increased inflow of fluids into the choroidal interstices due to blood flow congestion or a generalized thickening due to a tumour-induced inflammatory environment (Mitamura et al., 2022).

We observed more choroidal HRF in patients with AL than controls, which considerably reduced after disease remission. We speculate choroidal HRF represent a biomarker of leukaemic choroidopathy. Intraretinal HRF have been characterized in several diseases, such as diabetic macular oedema (Saurabh et al., 2021), angioid streaks (Romano et al., 2019) and age-related macular degeneration (Nassisi et al., 2018). Conversely, choroidal HRF have been seldom explored and have been interpreted as lipofuscin deposits (Piri et al., 2015; Saurabh et al., 2021), macrophages (Kim & Oh, 2022; Romano et al., 2020), degenerated RPE cells (Romano et al., 2020) or melanocytes (Kim & Oh, 2022). Hyperreflectivity on OCT is an optical property of different molecules, and we cannot univocally conclude on HRF composition. However, the integrity of the outer retinal layers and the dynamic changes of HRF in different AL stages may argue against degenerative changes (Piri et al., 2015). As leukocyte (especially macrophages) recruitment and activation occur in leukaemic niches (Ries et al., 2014), we speculate choroidal HRF may be leukaemic or inflammatory cells.

We did not find any difference in choriocapillaris FD density between AL and healthy eyes; similarly, the corrected FD density did not vary from the active to the remission phase of AL. These OCTA-based findings are consistent with the pathologic description from Allen & Straatsma (1961), who reported that choriocapillaris was uninvolved in patients with AL. We found an inverse correlation between choriocapillaris perfusion and the number of white blood cells. Assumptions on the relationship between choriocapillaris blood flow and systemic parameters are not straightforward, given the extensive interconnectivity of the choriocapillaris and the complex distribution of driving pressures and resistances throughout its network (Takita et al., 2018). However, we cannot exclude that the choriocapillaris perfusion was affected by hyperleukocytosis and blood flow disturbances due to the systemic condition (Cheung et al., 2021).

Only a few studies reported on the choroidal changes in blood dyscrasia. We also found an association between the choroidal thickness and the haemoglobin levels, in agreement with previous studies on patients with iron deficiency anaemia (Simsek et al., 2016) and β-thalassemia major (El-Shazly et al., 2016). We found an inverse association between the D-dimer and the choroidal vascularity in AL patients and a positive association between the D-dimer and the choroidal HRF count. Although a pro-coagulant state has been observed in patients with AL (Wang et al., 2018), it is difficult to hypothesize a comprehensive explanation combining choroidal vascular metrics (LCA and cFD density), the number of HRF and the D-dimer, and further research is warranted to confirm these putative associations.

This study has limitations, including the relatively small sample size and the lack of longitudinal analysis for all AL eyes. Our choroidal HRF quantification method required manual delineation of the choroidal area before imaging processing; automatic segmentation of the choroid and automated count of the HRF may improve the inter-rater reliability of the measurements. As we limited the analysis of the choriocapillaris FD density, the choroidal metrics and the choroidal HRF count to the central macula, widefield imaging could provide a more comprehensive picture of the degree of choroidal involvement in AL.

In conclusion, with the help of noninvasive multimodal imaging, we depicted in vivo the subclinical choroidal change in patients with AL, finding a predominant stromal involvement in the acute phase. We also identified choroidal HRF as a biomarker of leukaemic choroidopathy, and we hypothesized they could be leukocytes of either inflammatory or neoplastic origin. Choriocapillaris and choroidal vascularity correlated with a systemic procoagulant state, but further studies are needed to confirm and explain this relationship. Finally, a longer follow-up is warranted to elucidate the clinical value and the prognostic significance of leukaemic choroidopathy.

AUTHOR CONTRIBUTIONS

All the authors contributed to the conception or design of the work, the acquisition, analysis and interpretation of data, drafting the work, and revising it critically for important intellectual content. Each coauthor has seen and agrees with how his name is listed.

ACKNOWLEDGEMENT

Open access funding provided by BIBLIOSAN.

FUNDING INFORMATION

This research did not receive any specific grant from funding agencies in the public, commercial or not-for-profit sectors.

DISCLOSURES

Matteo Menean, Aurelio Apuzzo, Sara Mastaglio, Massimo Bernardi, Fabio Ciceri, Giulio Modorati, Elisabetta Miserocchi, Maria Vittoria Cicinelli: No financial disclosures. Francesco Bandello consultant for: AbbVie (North Chicago, Illinois, USA), Alimera (Alpharetta, Georgia, USA), Bayer Shering-Pharma (Berlin, Germany), Hoffmann-La-Roche (Basel, Switzerland), Novartis (Basel, Switzerland), Sanofi-Aventis (Paris, France), Thrombogenics (Heverlee, Belgium), Boehringer-Ingelheim (Ingelheim am Rhein, Germany), Fidia Sooft, Ntc Pharma, Sifi.

ORCID

Matteo Menean https://orcid.org/0000-0001-8512-2450
Francesco Bandello https://orcid.org/0000-0003-3238-9682
Maria Vittoria Cicinelli https://orcid.org/0000-0003-2938-0409

REFERENCES

Allen, R.A. & Straatsma, B.R. (1961) Ocular involvement in leukemia and allied disorders. *Archives of Ophthalmology*, 66, 490–508.

Bajenova, N.V., Vanderbeek, B.L. & Johnson, M.W. (2012) Change in choroidal thickness after chemotherapy in leukemic choroidopathy. *Retina*, 32, 203–205.

Bakst, R., Powers, A. & Yahalom, J. (2020) Diagnostic and therapeutic considerations for extramedullary leukemia. *Current Oncology Reports*, 22, 75.

Betzler, B.K., Ding, J., Wei, X., Lee, J.M., Grewal, D.S., Fekrat, S. et al. (2022) Choroidal vascularity index: a step towards software as a medical device. *British Journal of Ophthalmology*, 106, 149–155.

Borrelli, E., Abdelfattah, N.S., Uji, A., Nittala, M.G., Boyer, D.S. & Sadda, S.V.R. (2017) Postreceptor neuronal loss in intermediate age-related macular degeneration. *American Journal of Ophthalmology*, 181, 1–11.

Byon, I., Alagorie, A.R., Ji, Y., Su, L. & Sadda, S.R. (2020) Optimizing the repeatability of choriocapillaris flow deficit measurement from optical coherence tomography angiography. *American Journal of Ophthalmology*, 219, 21–32.

Cheung, C.M.G., Teo, K.Y.C., Tun, S.B.B., Busoy, J.M., Barathi, V.A. & Spaide, R.F. (2021) Correlation of choriocapillaris hemodynamic data from dynamic indocyanine green and optical coherence tomography angiography. *Scientific Reports*, 11, 15580.

Choi, Y.S. (2020) Recent advances in the management of primary central nervous system lymphoma. *Blood Research*, 55(S1), S58–S62.

Cicinelli, M.V., Mastaglio, S., Menean, M., Marchese, A., Miserocchi, E., Modorati, G. et al. (2022) Retinal microvascular changes in patients with acute leukemia. *Retina*, 42, 1762–1771.

Corradetti, G., Au, A., Borrelli, E., Xu, X., Bailey Freund, K. & Sarraf, D. (2019) Analysis of hyperreflective dots within the central fovea in healthy eyes using en face optical coherence tomography. *Investigative Ophthalmology & Visual Science*, 60, 4451.

Coupland, S.E. & Damato, B. (2008) Understanding intraocular lymphomas. *Clinical & Experimental Ophthalmology*, 36, 564–578.

Davis, J.L. (2013) Intraocular lymphoma: a clinical perspective. *Eye (Basingstoke)*, 27, 153–162.

Devine, S.M. & Larson, R.A. (1994) Acute leukemia in adults: recent developments in diagnosis and treatment. *CA: A Cancer Journal for Clinicians*, 44, 326–352.

Dick, J.E. & Lapidot, T. (2005) Biology of normal and acute myeloid leukemia stem cells. *International Journal of Hematology*, 82, 389–396.

El-Shazly, A.A.E.F., Elkitkat, R.S., Ebeid, W.M. & Deghedy, M.R. (2016) Correlation between subfoveal choroidal thickness and foveal thickness in thalassemic patients. *Retina*, 36, 1767–1772.

González-Herrero, I., Rodríguez-Hernández, G., Luengas-Martínez, A., Isidro-Hernández, M., Jiménez, R., García-Cenador, M. et al. (2018) The making of leukemia. *International Journal of Molecular Sciences*, 19(5), 1494.

Iovino, C., Pellegrini, M., Bernabei, F., Borrelli, E., Sacconi, R., Govetto, A. et al. (2020) Choroidal vascularity index: an in-depth analysis of this novel optical coherence tomography parameter. *Journal of Clinical Medicine*, 9(2), 595.

Kim, Y.H. & Oh, J. (2022) Hyperreflective foci in the choroid of normal eyes. *Graefe's Archive for Clinical and Experimental Ophthalmology*, 260, 759–769.

Koo, T.K. & Li, M.Y. (2016) A guideline of selecting and reporting intraclass correlation coefficients for reliability research. *Journal of Chiropractic Medicine*, 15, 155–163.

Leonardy, N.J., Rupani, M., Dent, G. & Klintworth, G.K. (1990) Analysis of 135 autopsy eyes for ocular involvement in leukemia. *American Journal of Ophthalmology*, 109, 436–444.

Mitamura, M., Kase, S., Hirooka, K., Endo, H., Ito, Y. & Cho, Y.I.S. (2022) Alterations of choroidal circulation and vascular morphology in a patient with chronic myeloid leukemia before and after chemotherapy. *BMC Ophthalmology*, 22, 160.

Nassisi, M., Fan, W., Shi, Y., Lei, J., Borrelli, E., Ip, M. et al. (2018) Quantity of intraretinal hyperreflective foci in patients with intermediate age-related macular degeneration correlates with 1-year progression. *Investigative Ophthalmology & Visual Science*, 59, 3431.

Nesper, P.L., Ong, J.X. & Fawzi, A.A. (2021) Exploring the relationship between multilayered choroidal neovascularization and choriocapillaris flow deficits in AMD. *Investigative Ophthalmology & Visual Science*, 62, 12.

Nicolini, N., Tombolini, B., Barresi, C., Pignatelli, F., Lattanzio, R. & Bandello, F.C.M.V. (2022) Assessment of diabetic choroidopathy using ultra-widefield optical coherence tomography. *Translational Vision Science & Technology*, 11(3), 35.

Piri, N., Nesmith, B.L.W. & Schaal, S. (2015) Choroidal hyperreflective foci in stargardt disease shown by spectral-domain optical coherence tomography imaging: correlation with disease severity. *JAMA Ophthalmology*, 133, 398–405.

Ries, C.H., Cannarile, M.A., Hoves, S. et al. (2014) Targeting tumor-associated macrophages with anti-CSF-1R antibody reveals a strategy for cancer therapy. *Cancer Cell*, 25(6), 846–859.

Romano, F., Arrigo, A., MacLaren, R.E., Charbel Issa, P., Birtel, J., Bandello, F. et al. (2020) Hyperreflective foci as a pathogenetic biomarker in choroideremia. *Retina*, 40(8), 1634–1640.

Romano, F., Mercuri, S., Arrigo, A., Marchese, A., Cicinelli, M.V., Albertini, G.C. et al. (2019) Identification of hyperreflective foci in angioid streaks. *Eye (Basingstoke)*, 33, 1916–1923.

Saurabh, K., Roy, R., Herekar, S., Mistry, S. & Choudhari, S. (2021) Validation of choroidal hyperreflective foci in diabetic macular edema through a retrospective pilot study. *Indian Journal of Ophthalmology*, 69, 3203–3206.

Simsek, A., Tekin, M., Bilen, A., Karadag, A.S., Bucak, I.H. & Turgut, M. (2016) Evaluation of choroidal thickness in children with iron deficiency anemia. *Investigative Ophthalmology & Visual Science*, 57, 5940.

Takita, A., Hashimoto, Y., Saito, W., Kase, S. & Ishida, S. (2018) Changes in blood flow velocity and thickness of the choroid in a patient with leukemic retinopathy. *American Journal of Ophthalmology Case Reports*, 12, 68–72.

Vieira, L., Silva, N.A., Medeiros, M.D., Flores, R. & Maduro, V. (2015) Acute lymphoblastic leukemia presenting with bilateral serous macular detachment. *Arquivos Brasileiros de Oftalmologia*, 78, 382–384.

Wang, P., Zhang, Y., Yang, H., Hou, W., Jin, B., Hou, J. et al. (2018) Characteristics of fibrinolytic disorders in acute promyelocytic leukemia. *Hematology*, 23, 756–764.

Zhang, Q., Shi, Y., Zhou, H., Gregori, G., Chu, Z., Zheng, F. et al. (2018) Accurate estimation of choriocapillaris flow deficits beyond normal intercapillary spacing with swept source OCT angiography. *Quantitative Imaging in Medicine and Surgery*, 8, 666.

SUPPORTING INFORMATION

Additional supporting information can be found online in the Supporting Information section at the end of this article.

How to cite this article: Menean, M., Apuzzo, A., Mastaglio, S., Bernardi, M., Ciceri, F., Modorati, G. et al. (2023) Imaging biomarkers of leukaemic choroidopathy. *Acta Ophthalmologica*, 00, 1–7. Available from: https://doi.org/10.1111/aos.15637